

# Matrix Metalloproteinase-7 Activation of Mouse Paneth Cell Pro- $\alpha$ -defensins

## SER<sup>43</sup> ↓ ILE<sup>44</sup> PROTEOLYSIS ENABLES MEMBRANE-DISRUPTIVE ACTIVITY\*

Received for publication, March 3, 2006, and in revised form, June 16, 2006. Published, JBC Papers in Press, July 5, 2006, DOI 10.1074/jbc.M602041200

Colby S. Weeks<sup>‡</sup>, Hiroki Tanabe<sup>§</sup>, Jason E. Cummings<sup>¶</sup>, Steve P. Crampton<sup>||</sup>, Tanya Sheynis<sup>\*\*</sup>, Raz Jelinek<sup>\*\*</sup>, T. Kyle Vanderlick<sup>¶</sup>, Melanie J. Cocco<sup>||</sup>, and Andre J. Ouellette<sup>‡††</sup>

From the Departments of <sup>‡</sup>Pathology & Laboratory Medicine, <sup>||</sup>Molecular Biology & Biochemistry, and <sup>††</sup>Microbiology & Molecular Genetics, and Center for Immunology, University of California, Irvine, California 92697-4800, the <sup>§</sup>Third Department of Internal Medicine, Asahikawa Medical College, Asahikawa, Hokkaido 078, Japan, the <sup>¶</sup>Department of Chemical Engineering, Princeton University, Princeton, New Jersey 08544, and the <sup>\*\*</sup>Department of Chemistry, Ben-Gurion University of the Negev, Beersheva 84105, Israel

Small intestinal Paneth cells secrete  $\alpha$ -defensin microbicial peptides as mediators of innate enteric immunity. In mice, production of mature Paneth cell  $\alpha$ -defensins, termed cryptdins (Crps), requires proteolytic activation of inactive precursors (pro-Crps) by the convertase matrix metalloproteinase-7. Proteolysis of mouse (pro-Crp4)<sup>20–92</sup> produces the specific cleavage intermediates pro-Crp4<sup>44–92</sup>, pro-Crp4<sup>54–92</sup>, and pro-Crp4<sup>59–92</sup>. To identify which cleavage event enables bactericidal activity, recombinant pro-Crp4-processing intermediates were purified to homogeneity and assayed for bactericidal peptide activity. The *in vitro* bactericidal activities of pro-Crp4-processing intermediates were very similar to fully processed Crp4, contrasting the lack of bactericidal and membrane-disruptive activity shown by pro-Crp4<sup>20–92</sup>. Thus, cleavage of pro-Crp4<sup>20–92</sup> at Ser<sup>43</sup> ↓ Ile<sup>44</sup> is sufficient to activate bactericidal activity, and amino acids in the pro-Crp4<sup>20–43</sup> of the proregion maintain the precursor in an inactive state. Because cationic Arg residues are determinants of Crp4 bactericidal peptide activity, we hypothesized that Asp and Glu residues in pro-Crp4<sup>20–43</sup> neutralize Crp4 Arg side chains in pro-Crp4<sup>20–92</sup>. Therefore, a pro-Crp4<sup>20–92</sup> variant with Gly substitutions at all pro-Crp4<sup>20–43</sup> Asp and Glu positions ((DE/G)-pro-Crp4) was prepared, and it was bactericidal and lysed phospholipid vesicles under conditions where native pro-Crp4<sup>20–92</sup> lacks activity. These findings show that MMP-7 proteolysis of pro-Crp4<sup>20–92</sup> at Ser<sup>43</sup> ↓ Ile<sup>44</sup> converts inactive precursors to bactericidal forms by removal of covalently associated, inhibitory acidic amino acids from proximity with the Crp4 component of the molecule.

Paneth cell  $\alpha$ -defensins contribute to innate mucosal immunity in the mammalian small intestine (1, 2). For example,  $\alpha$ -defensins account for ~70% of microbicidal peptide activity that is secreted from the base of small bowel crypts by mouse Paneth cells in response to cholinergic stimulation or exposure to bacteria and bacterial antigens (3). Defective dissolution of Paneth cell secretory granules in cystic fibrosis mice is associated with bacterial overgrowth, defective clearance of orally administered bacteria, and marked changes in the resident microflora (4, 5). Also, mice lacking matrix metalloproteinase-7 (MMP-7),<sup>2</sup> the mouse Paneth cell  $\alpha$ -defensin convertase (6, 7), have impaired immunity to oral bacterial infections (6). Further evidence implicating  $\alpha$ -defensins in Paneth cell secretions as mediators of innate enteric immunity derives from studies of mice transgenic for the human Paneth cell  $\alpha$ -defensin HD-5. The transgenic mice are immune to oral infection by *Salmonella enterica* serovar Typhimurium (*S. Typhimurium*), a highly virulent pathogen for wild-type mice (8). These considerations provide rationale for determining the mechanisms regulating the production and functional maturation of these peptide effectors.

Biosynthesis of  $\alpha$ -defensins requires post-translational activation of inactive proforms by lineage-specific proteinases (6, 9). Whether myeloid or Paneth cell in origin,  $\alpha$ -defensins are expressed as pre-propeptides consisting of co-translationally cleaved signal sequences, acidic prosegments, and an  $\alpha$ -defensin peptide localized in the C-terminal region of the precursor (10, 11). Human myeloid  $\alpha$ -defensins are processed within 4–24 h of synthesis by unknown proteinases to form major intermediates of 75 and 56 amino acids (12). Expression of

\* This work was supported by National Institutes of Health Grant DK044632 (to A. J. O.), the Human Frontiers Science Program (to A. J. O. and R. J.), the U.S.-Israel Binational Science Foundation (to R. J. and A. J. O.), and the University of California, Irvine Academic Senate Council on Research, Computing, and Library Resources (to M. J. C.). The costs of publication of this article were defrayed in part by the payment of page charges. This article must therefore be hereby marked "advertisement" in accordance with 18 U.S.C. Section 1734 solely to indicate this fact.

<sup>†</sup> To whom correspondence should be addressed: Dept. of Pathology & Laboratory Medicine, Med. Sci. D440, School of Medicine, College of Health Sciences, University of California, Irvine, CA 92697-4800. Tel.: 949-824-4647; Fax: 949-824-1098; E-mail: aouellet@uci.edu.

<sup>2</sup> The abbreviations used are: MMP-7, matrix metalloproteinase 7; Crp4, cryptdin-4<sup>91–92</sup>; pro-Crp4, procryptdin-4<sup>20–92</sup>; *S. Typhimurium*, *Salmonella enterica* serovar Typhimurium; HD-5, human defensin-5; HNP-1, human neutrophil peptide-1; (DE/G)-pro-Crp4, (D20G/D26G/E27G/E28G/E32G/E33G/E37G/E38G/D39G)-pro-Crp4<sup>20–92</sup>; AU-PAGE, acid-urea-polyacrylamide gel electrophoresis; MALDI-TOF MS, matrix-assisted laser desorption ionization time-of-flight mass spectrometry; TSB, Trypticase soy broth; PIPES, 1,4-piperazinediethanesulfonic acid; DMPC, dimyristoylphosphatidylcholine; DMPG, dimyristoylphosphatidylglycerol; PDA, polydiacetylene; LUV, large unilamellar phospholipid vesicles; ANTS, 8-aminonaphthalene-1,3,6-trisulfonic acid; DPX, *p*-xylenebispyrindinium bromide; ONPG, 2-nitrophenyl  $\beta$ -D-galactopyranoside; percent colorimetric response; NOESY, nuclear Overhauser effect spectroscopy; TOCSY, total correlation spectroscopy; DQF-COSY, double quantum-filtered correlation spectroscopy.

human neutrophil  $\alpha$ -defensin pro-HNP-1 with targeted proregion deletions impaired pro-HNP-1 processing in mouse 32D cl3 cells (13). In contrast, human Paneth cells store and secrete unprocessed pro- $\alpha$ -defensins, which are activated by anionic and meso trypsin isoforms that co-localize with HD-5 in secretory granules (9). Trypsin cleaves pro-HD-5 at Arg<sup>55</sup> ↓ Ala<sup>56</sup> and Arg<sup>62</sup> ↓ Thr<sup>63</sup> to produce mature HD-5, with Arg<sup>55</sup> ↓ Ala<sup>56</sup> proteolysis inducing activation. In mice, all Paneth cell pro-Crps investigated are processed by MMP-7 cleavage at three conserved sites: Ser<sup>43</sup> ↓ Ile/Val<sup>44</sup>, Ala<sup>53</sup> ↓ Leu<sup>54</sup>, and Ser<sup>58</sup> ↓ Leu<sup>59</sup>, which activates bactericidal activity and enables membrane disruptive activity (14, 15).

The bactericidal activity of mouse Paneth cell  $\alpha$ -defensins, termed cryptidins (Crps), correlates directly with the ability to interact with and disrupt membranes. Most  $\alpha$ -defensins kill bacterial cell targets by membrane disruption, although individual peptides differ in their mechanisms of action as shown by studies with model membrane systems *in vitro* (16, 17). Crp4, the most bactericidal of the known mouse  $\alpha$ -defensins, binds to biomimetic phospholipid membranes (18) and induces graded solute leakage from model membrane vesicles (19). In addition, the bactericidal activities of attenuated Crp4 peptide variants correspond directly with their *in vitro* membrane-disruptive activities (19, 20). Full-length pro-Crp4<sup>20-92</sup> lacks bactericidal activity *in vitro* (14), and the molecule binds poorly and induces only modest vesicle lysis (18, 20). These findings show that the potent membrane disruptive behavior of mature Crp4 remains inactive in pro-Crp4<sup>20-92</sup> until MMP-7 proteolysis cleavage enables binding and lysis of target cell membranes (9, 14). To identify which cleavage event activates pro-Crp4, recombinant pro-Crp4-processing intermediates were prepared and tested for bactericidal and membrane-disruptive capabilities.

Here, we report that the Ser<sup>43</sup> ↓ Ile<sup>44</sup> cleavage event is sufficient to convert inactive pro-Crp4 to a fully functional state, despite the presence of a 17-amino acid N-terminal extension. Furthermore, 9 acidic amino acid residue positions in pro-Crp4<sup>20-43</sup> of the proregion are shown to maintain pro-Crp4 in an inactive state prior to MMP-7 proteolysis at Ser<sup>43</sup> ↓ Ile<sup>44</sup>.

## EXPERIMENTAL PROCEDURES

**Preparation of Crp4 and Pro-Crp4**—Recombinant Crp4 and pro-Crp4 were expressed in *Escherichia coli* as N-terminal His<sub>6</sub>-tagged fusion proteins from the pET-28a expression vector (Novagen, Inc., Madison, WI) at the EcoRI and Sall sites as described (14, 18). Crp4 cDNA (accession number NM\_010039) was used as template to amplify sequences for cloning using forward primer EcoRI-Met-Crp4-f (5'-GCGCG AATTC ATCGA GGGAA GGATG GGT TT GTTAT GCTAT GT-3') paired with reverse primer Crp4-Stop-Sall-r (5'-TATGT CGACT CAGCG GCGGG GGCAG CAGT-3'). For pro-Crp4, forward primer EcoRI-Met-PC4-f (5'-GCGCG AATTC ATGGA TCCTA TCCAA AACAC A-3') and reverse primer Crp4-Stop-Sall-r (5'-TATGT CGACT CAGCG GCGGG GGCAG CAGT-3') were used. The underlined codons in forward primers denote Met codons introduced to provide a cyanogen bromide cleavage site at the N termini of all expressed peptides (14, 18). PCR was performed using GeneAMP PCR Core Reagents (Applied Biosystems, Foster

City, CA) by incubating the reaction mixture for 94 °C for 5 min followed by 30 cycles of 94 °C for 30 s, 60 °C for 30 s, and 72 °C for 30 s followed by an extension reaction for 7 min at 72 °C. The amplimers were cloned in pCR-2.1 TOPO (Invitrogen), verified by DNA sequencing, excised with EcoRI and Sall, and subcloned into pET-28a plasmid DNA (Novagen). Plasmids were transfected into *E. coli* BL21-CodonPlus (DE3)-RIL (Stratagene, La Jolla, CA) for expression.

**Preparation of Pro-Crp4-processing Intermediates**—The pro-Crp4<sup>44-92</sup>- and pro-Crp4<sup>54-92</sup>-processing intermediates were amplified from a pro-Crp4 cDNA clone in the pET-28a vector (14). The pro-Crp4<sup>44-92</sup> coding sequence was amplified using forward primer EcoRI-Met-44-PC4-F (5'-ATATA TGAAT TCATG ATCTC CTTTG GAGGC-3') and reverse primer Crp4-Stop-Sall-r (5'-TATGT CGACT CAGCG GCGGG GGCAG CAGT-3'). The pro-Crp4<sup>54-92</sup> cDNA was amplified using forward primer EcoRI-Met-54-PC4-F (5'-ATATA TGAAT TCATG CTTCA TGAAA AATCT-3') and reverse primer Crp4-Stop-Sall-r. The amplimers were prepared for fusion peptide expression, as discussed in the previous section (14, 18).

**Mutagenesis of Asp and Glu Residues in Pro-Crp4<sup>20-43</sup>**—All codons corresponding to Asp and Glu in the first 24 amino acids of pro-Crp4<sup>20-92</sup> were substituted with Gly codons in a series of mutagenizing PCR reactions to prepare (D20G/D26G/E27G/E28G/E32G/E33G/E37G/E38G/D39G)-pro-Crp4 ((DE/G)-pro-Crp4). The cDNA template for the first reaction was a pro-Crp4 clone in the pET-28a vector; the forward primer was PC4-DE/G-1-F (5'-CAGCC AGGAG GAGGA GGACA GGCTG TGTCT ATCTC CTTT-3'), and the reverse primer was Crp4-Stop-Sall-r (5'-TATGT CGACT CAGCG GCGGG GGCAG CAGT-3'). Each successive reaction used the amplification product from the previous reaction as a template using a forward mutagenizing primer that overlapped the 5'-end of the template and contained additional 5'-overhanging codons to extend the sequence. The same Crp4-Stop-Sall-r reverse primer was used in each PCR reaction. The forward primers of the second and third PCR reactions were PC4-DE/G-2-F (5'-GGAAC TAATA CTGGA GGACA GCCAG GAGGA GGA-3') and PC4-DE/G-3-F (5'-ATCCA AAACA CAGGA GGAGGA ACTAA TACTG GA-3'), respectively. The forward primer, PC4-DE/G-F (5'-GCGCG AATTC ATGGG ACCTA TCCAA AACAC A-3'), was paired with the reverse primer Crp4-Stop-Sall-r in the final PCR reaction. The amplimer was prepared for fusion peptide expression, as discussed in the previous section (14, 18).

**Preparation of Recombinant Proteins**—Recombinant proteins were expressed as His<sub>6</sub>-tagged peptides and purified to homogeneity. Expression was induced by 0.1 mM isopropyl- $\beta$ -D-1-thiogalactopyranoside for 6 h at 37 °C in Terrific Broth medium (19). Cells were lysed by sonication in 6 M guanidine-HCl, 100 mM Tris-HCl (pH 8.0) and clarified by centrifugation (14, 18). The His<sub>6</sub>-tagged fusion peptides were affinity purified by nickel-nitrilotriacetic acid resin affinity chromatography and eluted with 1 M imidazole, 6 M guanidine-HCl, 100 mM Tris-HCl (pH 5.9) (14). Fusion proteins were reacted with 10 mg/ml CNBr in 80% formic acid for 18 h at 25 °C, diluted with water, and lyophilized. Cleavage products were resuspended in

5% acetic acid and were separated by C18 reversed-phase high-pressure liquid chromatography with a gradient of acetonitrile with 0.1% trifluoroacetic acid as an ion-pairing agent. Peptide homogeneity was confirmed by analytical AU-PAGE, and the molecular masses were determined by matrix-assisted laser desorption ionization mode mass spectrometry (Voyager-DE MALDI-TOF, PE-Biosystems, Foster City, CA).

**Bactericidal Peptide Assays**—The bactericidal activity of purified recombinant peptides was tested against *E. coli* ML35, *Staphylococcus aureus* 502A, *Vibrio cholerae*, *Listeria monocytogenes* 104035, and *Salmonella enterica* serovar Typhimurium strains. Bacteria growing exponentially in Trypticase soy broth (TSB) at 37 °C were collected by centrifugation, washed, and resuspended in 10 mM PIPES (pH 7.4) supplemented with 0.01 volume (1% v/v) TSB (PIPES-TSB) (14, 18). Bacteria ( $5 \times 10^6$ /ml) were exposed to varied peptide concentrations for 1 h at 37 °C in 50  $\mu$ l of PIPES-TSB. Samples were diluted 1:100 with 10 mM PIPES (pH 7.4) and plated on Trypticase soy agar plates using an Autoplate 4000 (Spiral Biotech Inc., Bethesda, MD). Surviving bacteria were quantified as colony forming units (CFUs) per milliliter after 10–18 h of incubation.

**MMP-7 Digestion of Recombinant Peptides**—Crp4, pro-Crp4, and (DE/G)-pro-Crp4 (10  $\mu$ g) were incubated with or without 0.5 M equivalents of MMP-7 in 1/10 HEPES buffer (1 mM HEPES, 15 mM NaCl, 0.5 mM CaCl<sub>2</sub>, pH 7.4) for 18 h at 37 °C. Samples (700  $\mu$ mol) of each peptide were used in bactericidal assays already described, and the remaining material was analyzed by AU-PAGE.

**Peptide Interactions with Phospholipid/Polydiacetylene-mixed Vesicles**—Recombinant Crp4, pro-Crp4, pro-Crp4<sup>44–92</sup>, pro-Crp4<sup>54–92</sup>, and (DE/G)-pro-Crp4 were assayed for the membrane interaction activities. Vesicles consisting of dimyristoylphosphatidylcholine (DMPC), dimyristoylphosphatidylglycerol (DMPG), and polydiacetylene (PDA) (1:1:3 molar ratio) were prepared as described previously (18). Phospholipids (Sigma) and 10,12-tricosadiynoic acid monomer (GFS Chemicals, Powell, OH) were dissolved in chloroform/ethanol (1:1) and dried together *in vacuo* to constant weight. The lipid film was suspended in deionized water, probe-sonicated for 3 min at 70 °C, and incubated overnight at 4 °C. PDA was polymerized by irradiation at 254 nm for 30 s, producing suspensions with an intense blue appearance. Peptides at concentrations varying from 0.2 to 3  $\mu$ M were added to 60  $\mu$ l of vesicle solutions (0.5 mM total lipid) in 25 mM Tris-base (pH 8.0), diluted to 1 ml by deionized water, and spectra were acquired at 28 °C between 400 and 700 nm on a Jasco V-550 spectrophotometer (Jasco Corp., Tokyo, Japan) using a 1-cm optical path cell. Blue-red color transitions within the vesicle solutions, defined as the percent colorimetric response (%CR), were calculated as described previously (18, 21). Ultracentrifugation binding assays were performed to evaluate peptide affinities for the vesicles (18).

**Peptide Interactions with Large Unilamellar Vesicles**—Recombinant pro-Crp4 and peptide variants were investigated for the ability to induce leakage from large unilamellar phospholipid vesicles (LUV) of defined composition. LUV of palmitoylphosphatidylglycerol (Avanti Polar Lipids, Birmingham, AL) were loaded with a fluorophore/quencher system (22,

23). Aqueous lipid solutions consisting of 17 mM 8-aminonaphthalene-1,3,6-trisulfonic acid (ANTS, Molecular Probes, Eugene, OR), 60.5 mM *p*-xylenebispyridinium bromide (DPX, Molecular Probes), 10 mM HEPES, 31 mM NaCl, and 19.5 mM NaOH (260 mosM/liter, pH 7.4) were vortexed, frozen, and thawed for 5 cycles and then extruded through polycarbonate filters with 100 nm pores. Vesicles were separated from unencapsulated ANTS/DPX by gel-permeation chromatography with 130 mM NaCl, 10 mM HEPES, and 4.5 mM NaOH (260 mosM/liter, pH 7.4) as column eluant. Vesicular suspensions diluted with eluant buffer to  $\sim$ 74  $\mu$ M of total lipid were incubated with peptides at ambient temperature. Time-dependent fluorescence produced by ANTS release was monitored at 520 nm (excitation at 353 nm) as described previously (19, 22). The kinetics of vesicular leakage was a function of peptide concentration, and equilibrium was attained  $\leq$ 4 h. Thus, 4-h values were expressed relative to fluorescence obtained by vesicular solubilization with Triton X-100.

***E. coli* ML35 Permeabilization Measured by ONPG Conversion**—Exponentially growing *E. coli* ML35 cells were washed and resuspended in 10 mM PIPES-TSB. Bacteria were exposed in triplicate to Crp4, pro-Crp4, pro-Crp4<sup>44–92</sup>, pro-Crp4<sup>54–92</sup>, and (DE/G)-pro-Crp4 in the presence of 2.5 mM ONPG for 2 h at 37 °C. *E. coli* ML35, which express  $\beta$ -galactosidase constitutively and are permease-negative, does not take up ONPG unless permeabilized by external factors, such as defensins.  $\beta$ -Galactosidase hydrolysis of ONPG was measured at 405 nm on a 96-well Spectra-Max plate spectrophotometer (Molecular Devices, Sunnyvale, CA).

**NMR Assay of Defensin Structure**—Pro-Crp4<sup>20–92</sup>, pro-Crp4<sup>44–92</sup>, pro-Crp4<sup>54–92</sup>, and (DE/G)-pro-Crp4<sub>92</sub> were lyophilized and dissolved in 90% H<sub>2</sub>O/10% D<sub>2</sub>O or D<sub>2</sub>O at final protein concentrations between 300  $\mu$ M and 1 mM. NMR data were collected on a Varian Inova 800-MHz spectrometer. Nuclear Overhauser effect spectroscopy (NOESY,  $\tau_m$  200 and 300 ms), total correlation spectroscopy (TOCSY,  $\tau_m$  45 ms), and double quantum-filtered correlation spectroscopy (DQF-COSY) experiments were performed. The water signal was eliminated using WATERGATE (24). In each case, 1024  $\times$  256 complex points were collected and shifted, sine-squared apodization and zero-filling to twice the data size were applied prior to Fourier transform. Data were processed using NMRPipe (25) and were analyzed using Sparky (www.cgl.ucsf.edu/home/sparky/). Assignments for Crp4 from a previous study (26) were confirmed and compared with those of pro-Crp4<sup>20–92</sup>, pro-Crp4<sup>44–92</sup>, pro-Crp4<sup>54–92</sup>, and (DE/G)-pro-Crp4.

## RESULTS

**Disulfide Arrays of Recombinant Peptides**—Pro-Crp4<sup>44–92</sup> and pro-Crp4<sup>54–92</sup> are pro-Crp4 variants with N termini that correspond to the canonical MMP-7-catalyzed cleavage events at Ser<sup>43</sup>  $\downarrow$  Ile<sup>44</sup> and Ala<sup>53</sup>  $\downarrow$  Leu<sup>54</sup> (14) (Fig. 1A). The pro-Crp4-processing intermediates were purified to homogeneity by C18 reversed-phase high-pressure liquid chromatography, which was verified by AU-PAGE analysis (Fig. 1B), and peptide masses were confirmed by MALDI-TOF mass spectrometry (not shown).

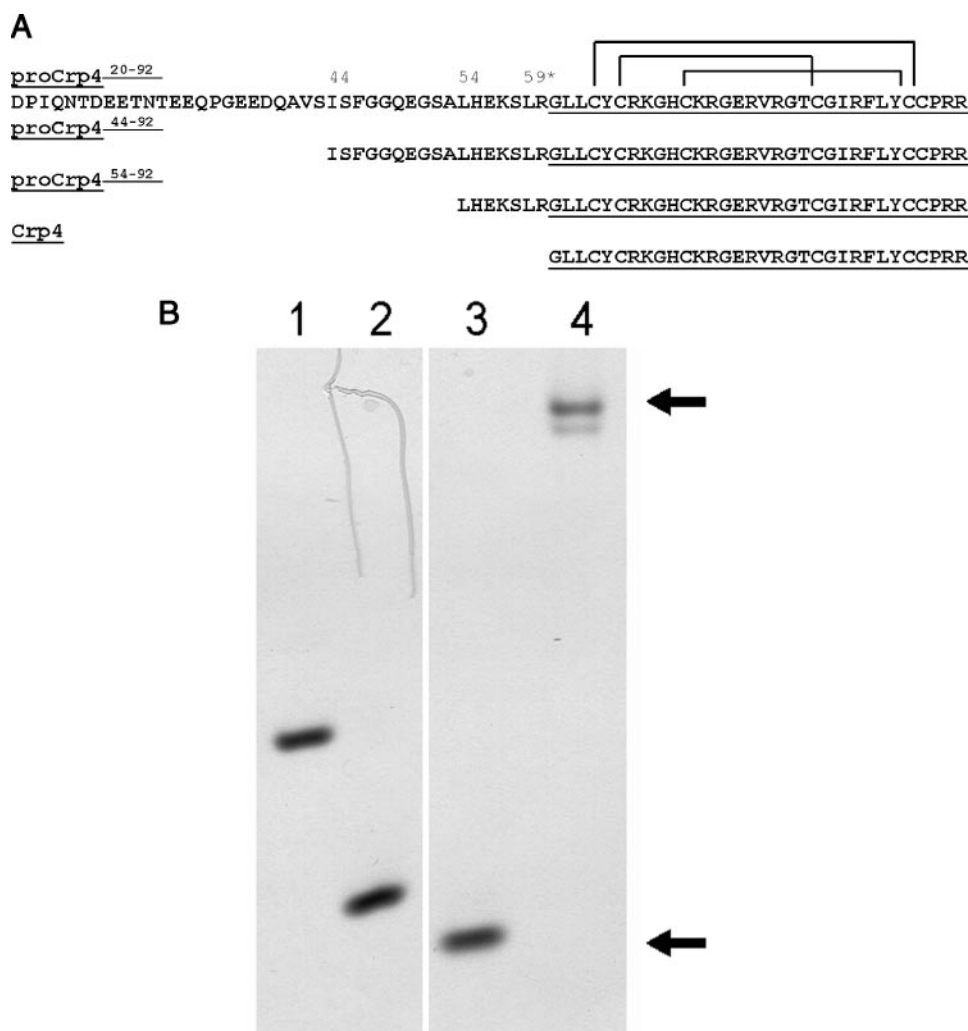


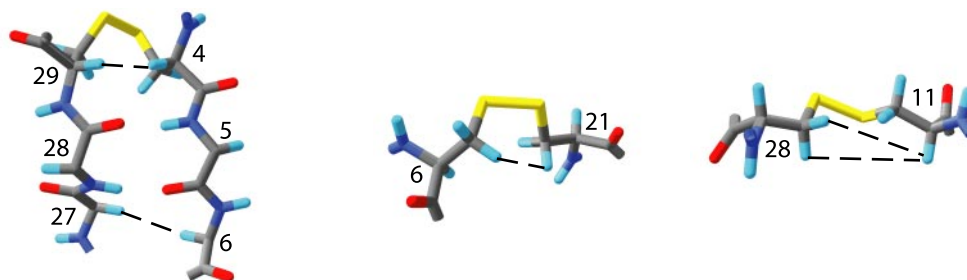
FIGURE 1. Recombinant pro-Crp4<sup>20-92</sup>, pro-Crp4-processing intermediates, and Crp4. *A*, the primary structures of the recombinant peptides prepared and assayed are shown. The numerals 44, 54, and 59 denote the sites of MMP-7-mediated cleavage of pro-Crp4<sup>20-92</sup>. The asterisk denotes the native N terminus of Crp4 detected *in vivo*, and the underlining in each sequence signifies the fully processed native Crp4 sequence. The disulfide connectivities are identified by the connecting bars above the pro-Crp4<sup>20-92</sup> sequence. *B*, 5- $\mu$ g samples of recombinant peptides depicted in *A* were resolved by AU-PAGE and stained with Coomassie Blue. Lanes: 1, pro-Crp4<sup>44-92</sup>; 2, pro-Crp4<sup>54-92</sup>; 3, Crp4 (lower arrow) and pro-Crp4<sup>20-92</sup> (upper arrow).

Pro-Crp4<sup>20-92</sup>, pro-Crp4<sup>44-92</sup>, and pro-Crp4<sup>54-92</sup> molecules were shown to have correct C<sup>I</sup>-C<sup>VI</sup>, C<sup>II</sup>-C<sup>IV</sup>, and C<sup>III</sup>-C<sup>V</sup> disulfide connectivities by NMR spectrometry (Fig. 2), ruling out the possibility that peptide bactericidal activities could result from disrupted  $\alpha$ -defensin cysteine pairings. Sequential assignments were made through each strand of the beta sheet using NOESY and TOCSY CH <sub>$\alpha$</sub> -NH connectivities. DQF-COSY and TOCSY data were used to determine the identity of each spin system and confirm backbone assignments. Sections of NOESY spectra that include the cysteine side chain  $\alpha$  and  $\beta$  protons for pro-Crp4<sup>20-92</sup>, pro-Crp4<sup>44-92</sup>, pro-Crp4<sup>54-92</sup>, and (DE/G)-pro-Crp4 (Fig. 2) confirmed that the disulfide connectivities correspond to those of native  $\alpha$ -defensins. In addition, analysis of backbone NOEs demonstrates existence of a  $\beta$ -strand conformation with a register identical to that of Crp4. Therefore, all recombinant peptides investigated in these experiments were confirmed by NMR to contain trisulfide arrays characteristic of  $\alpha$ -defensins.

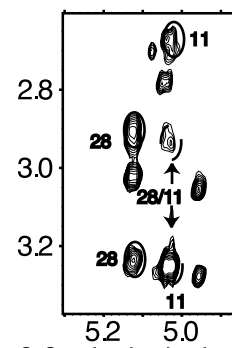
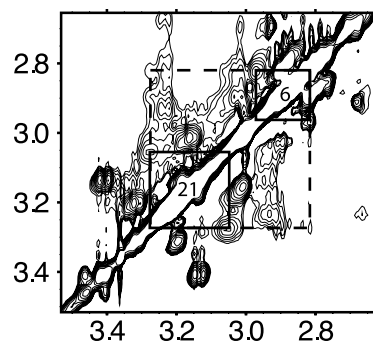
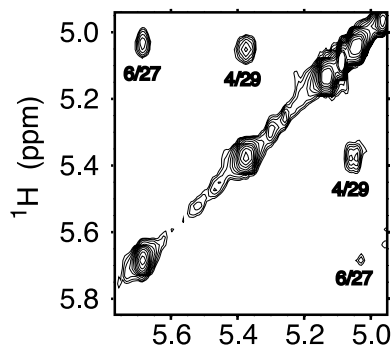
*MMP-7 Proteolysis of Pro-Crp4 at Ser<sup>43</sup> ↓ Ile<sup>44</sup> Confers Bactericidal Activity*—The activating cleavage event in pro-Crp4 processing was determined by analysis of recombinant pro-Crp4-processing intermediates. At 3  $\mu$ M final peptide concentration, pro-Crp4<sup>44-92</sup> and pro-Crp4<sup>54-92</sup> and Crp4 had equivalent bactericidal activities in *in vitro* bactericidal assays against *E. coli* ML35, *V. cholerae*, *S. aureus* 502a, *L. monocytogenes*, and *S. Typhimurium*  $\Delta$ *phoP*. The biological variability evident in bactericidal assays at low peptide concentrations may be due to steric effects of the N-terminal extensions in the pro-Crp4<sup>44-92</sup> and pro-Crp4<sup>54-92</sup> molecules. Characteristically (14), pro-Crp4<sup>20-92</sup> was inactive or markedly less active than all peptides assayed at concentrations tested. The relative bactericidal activities shown in Fig. 3 against *S. aureus* 502A, *L. monocytogenes*, and *S. Typhimurium*  $\Delta$ *phoP* are representative of results for all bacteria assayed. The fact that the processing intermediates are as active as Crp4 and that native pro-Crp4<sup>20-92</sup> lacks activity in these assays shows that all MMP-7-mediated cleavage events activate pro-Crp4. More importantly, however, the findings show that proteolysis at Ser<sup>43</sup> ↓ Ile<sup>44</sup>, the cleavage step farthest from the Crp4 N terminus, is sufficient to induce full bactericidal activity. It follows that amino acids located between Asp<sup>20</sup> and Ser<sup>43</sup>

must contribute to maintaining pro-Crp4 in an inactive state prior to conversion by MMP-7.

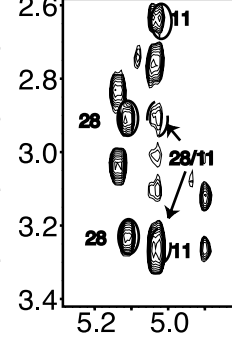
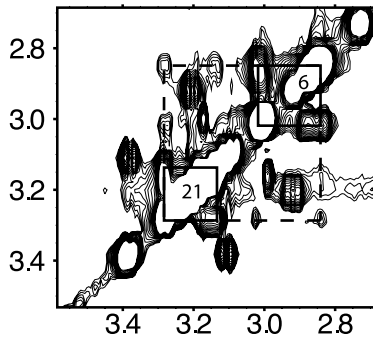
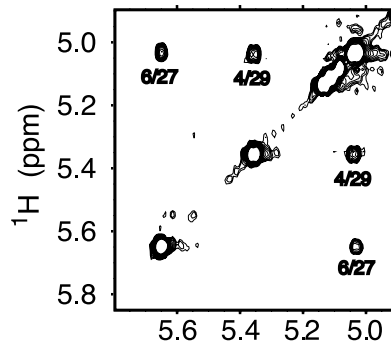
*Membrane Binding and Disruption by Pro-Crp4-processing Intermediates*—The mechanisms of pro-Crp4<sup>44-92</sup> and pro-Crp4<sup>54-92</sup> bactericidal action were investigated by measuring peptide binding to lipid/PDA-mixed vesicles and peptide-induced leakage from LUVs relative to Crp4 and native pro-Crp4<sup>20-92</sup>. Previous studies have shown that phospholipid/PDA assemblies undergo rapid blue-red chromatic transformations induced by interactions with membrane-active peptides (18, 21, 27), and peptides that localize at the lipid/water interface of the membrane bilayer induce stronger surface perturbations and greater %CR values than peptides that insert into the hydrophobic bilayer core (18, 21). Pro-Crp4<sup>44-92</sup>, pro-Crp4<sup>54-92</sup>, and mature Crp4 caused similar colorimetric dose-response curves, reaching maximum %CR values of  $\sim$ 40% (Fig. 4A). Therefore, these three peptides interact comparably with the phospholipid head-group



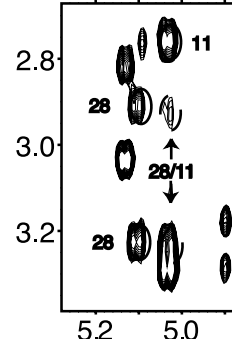
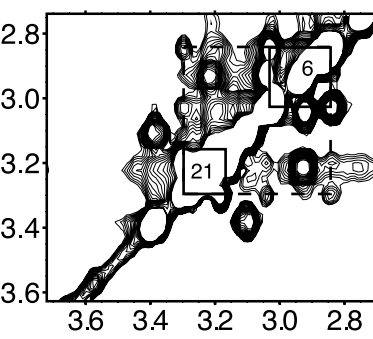
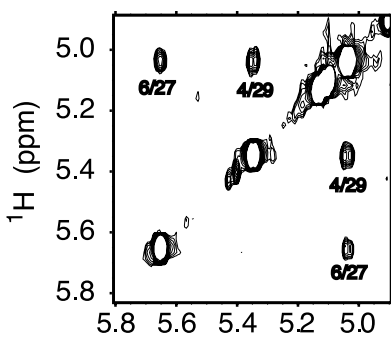
proCrp4



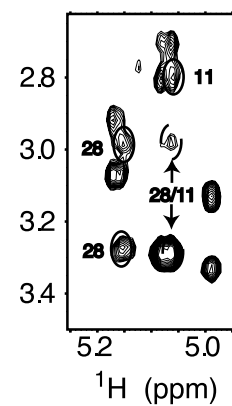
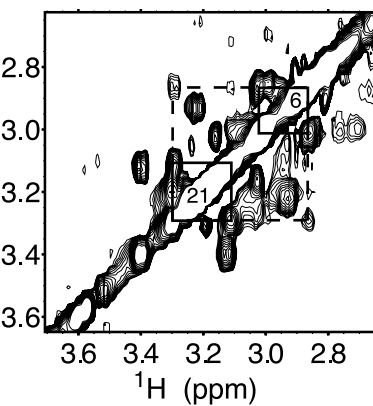
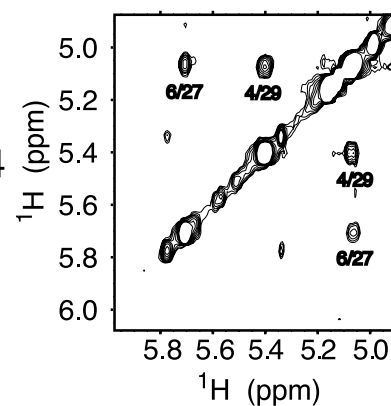
proCrp4<sup>44-92</sup>



proCrp4<sup>54-92</sup>



(DE/G)-proCrp4



region of vesicles, disrupting membranes to similar extents (18). In contrast, native pro-Crp4<sup>20-92</sup> interacts only weakly with lipid/PDA vesicles as the low colorimetric response indicates (Fig. 4A), again as previously shown (18). Overall, the lipid/PDA binding results are consistent with peptide-induced LUV leakage assays (Fig. 4B) and with relative *in vitro* bactericidal peptide activities (Fig. 3). Also, these experiments confirm that Crp4 and pro-Crp4 intermediates have similar membrane-binding and disruptive activities in contrast to full-length pro-Crp4<sup>20-92</sup>, which interacts poorly with lipid vesicles. The bactericidal activities of Crp4 and Crp4 mutants correlate well with the membrane-perturbing activity of the peptides in vesicle leakage assays (19, 20).

To test the hypothesis that bactericidal pro-Crp4-processing intermediates act by membrane-perturbing mechanisms, peptide-induced vesicle leakage was measured and compared with the activities of pro-Crp4<sup>20-92</sup> and Crp4 (19, 20). Mature Crp4 induces extensive leakage from ANTS/DPX-loaded anionic LUV (23), but native pro-Crp4<sup>20-92</sup> has only slight membrane-disruptive capability (Fig. 4B). Consistent with their bactericidal activities, pro-Crp4-processing intermediates perturbed LUV membranes more than pro-Crp4<sup>20-92</sup> (Fig. 4B), although the extent of pro-Crp4<sup>44-92</sup> and pro-Crp4<sup>54-92</sup> induced leakage was slightly less than that of mature Crp4. These results support the conclusion that Ser<sup>43</sup> ↓ Ile<sup>44</sup> proteolysis enables or facilitates increased interactions between these peptides and phospholipid vesicles. Because the bactericidal and membrane-disruptive activities of Crp4 depend, in part, on cationic Arg residues (20), we considered that the Ser<sup>43</sup> ↓ Ile<sup>44</sup> cleavage event may activate pro-Crp4<sup>20-92</sup> by eliminating steric hindrance or charge neutralization imposed by the electronegative pro-Crp4<sup>20-43</sup> region.

**Acidic Amino Acids in Pro-Crp4<sup>20-43</sup> Block Pro-Crp4 Bactericidal Activity**—To investigate mechanisms that maintain pro-Crp4 in an inactive state, we hypothesized that dissociated carboxyl groups of Asp and Glu side chains in pro-Crp4<sup>20-43</sup> interact with Arg guanidinium side chains when the pro-Crp4<sup>20-43</sup> region is bound covalently to the precursor. If so, the electropositive Crp4 peptide surface that interacts with phospholipid head groups in the bacterial cell envelope would be neutralized, preventing membrane binding. To test whether the anionic Asp and Glu residues in pro-Crp4<sup>20-43</sup> do inhibit pro-Crp4<sup>20-92</sup> antibacterial action, a recombinant pro-Crp4<sup>20-92</sup> variant with Gly substitutions at all Asp and Glu residues in pro-Crp4<sup>20-43</sup> ((DE/G)-pro-Crp4) was prepared (Fig. 5A). (DE/G)-pro-Crp4 peptide homogeneity was assessed by reversed-phase high-pressure liquid chromatography and by AU-PAGE (Fig. 5B), and its mass was confirmed by MALDI-TOF MS (not shown).

Because bactericidal activity could potentially result from artifacts of peptide misfolding, NMR experiments were per-

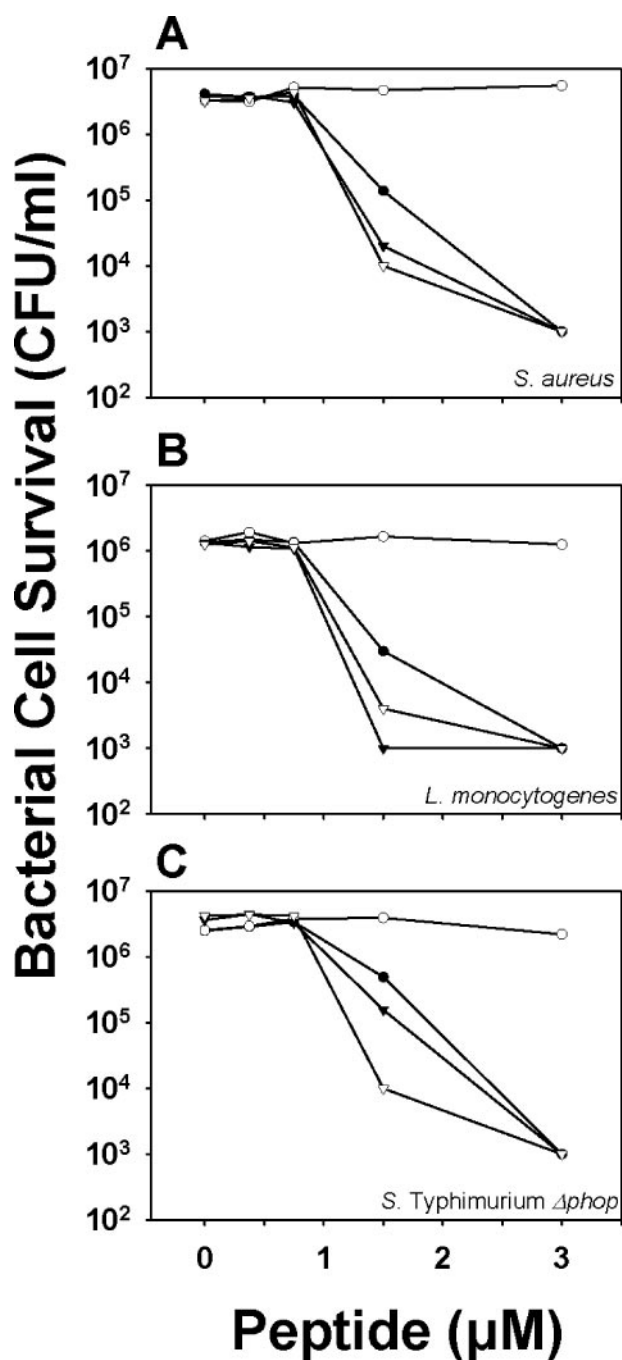
formed on (DE/G)-pro-Crp4 to determine the disulfide connectivities. Sections of NOESY spectra that include the cysteine side-chain  $\alpha$  and  $\beta$  protons (Fig. 2) confirmed that the trisulfide arrays of pro-Crp4<sup>20-92</sup>, pro-Crp4<sup>44-92</sup>, pro-Crp4<sup>54-92</sup>, and (DE/G)-pro-Crp4 are the same as that of native Crp4. A comparison of chemical shifts of backbone NH groups shows that there are no differences >0.05 ppm between (DE/G)-pro-Crp4 and Crp4 resonances. Thus, the Crp4 domain in (DE/G)-pro-Crp4 is correctly folded.

The effects of Asp and Glu residue positions on the inhibition of pro-Crp4<sup>20-92</sup> bactericidal activity were inferred by determining the *in vitro* bactericidal peptide activity of (DE/G)-pro-Crp4. Assays performed against Gram-positive and Gram-negative bacterial species showed that deleting acidic side chains in pro-Crp4<sup>20-43</sup> produced a (DE/G)-pro-Crp4 molecule with the same antibacterial activity as Crp4 (Fig. 6), particularly at high peptide concentrations. Assay variability increased at low peptide levels, perhaps due to steric effects of the 39-amino acid (DE/G)-pro-Crp4 N-terminal extension or some yet undefined structural factor. These findings do not rule out possible inhibitory contributions of additional prosegment amino acid residues that remained unchanged in (DE/G)-pro-Crp4. Despite the presence of a full-length, though charge-modified, prosegment, (DE/G)-pro-Crp4 was lethal to bacteria (Fig. 6). Native pro-Crp4<sup>20-92</sup> was predictably inactive at almost all concentrations tested, except for low pro-Crp4 activity observed at 15 mM of peptide.

These experiments also demonstrate that variant Crp4 molecules, even molecules with as many as 41 amino acids extending beyond the natural  $\alpha$ -defensin N terminus, retain bactericidal activity when the defensin fold is correct and peptide charge is not neutralized by residues in the proregion. Furthermore, this biochemical evidence supports the conclusion that the Asp and Glu residues in pro-Crp4<sup>20-43</sup> maintain native pro-Crp4<sup>20-92</sup> in an inactive state until MMP-7 catalyzes the Ser<sup>43</sup> ↓ Ile<sup>44</sup> cleavage.

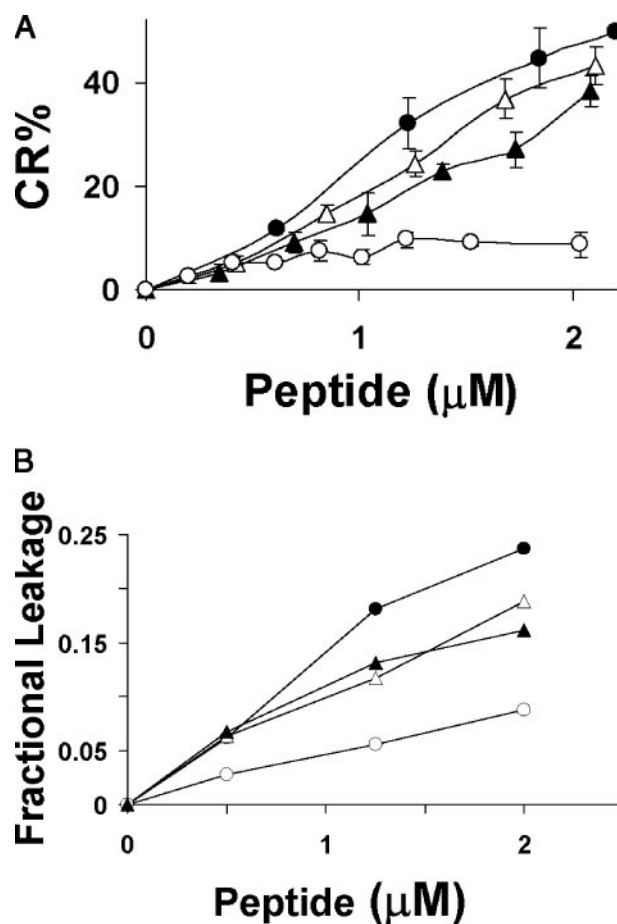
**(DE/G)-pro-Crp4 Binds to Membrane Vesicles and Disrupts Model Membranes**—Studies of many Crp4 peptide variants have shown a direct correspondence between relative peptide bactericidal activity and an ability to bind to and induce leakage from model membrane vesicles. To test whether (DE/G)-pro-Crp4 bactericidal action correlates similarly with membrane-disruptive behavior, peptide binding to phospholipid/PDA vesicles and peptide-induced LUV leakage were assayed and compared with native Crp4 and pro-Crp4<sup>20-92</sup> (Fig. 7). Replacement of pro-Crp4<sup>20-43</sup> Asp and Glu residues with Gly markedly improved the association of pro-Crp4<sup>20-92</sup> with lipid/PDA vesicles, as evident from the 30% difference in %CR plateaus of native pro-Crp4<sup>20-92</sup> and (DE/G)-pro-Crp4 (Fig. 7A). Unlike nominally inactive pro-Crp4<sup>20-92</sup>, (DE/G)-pro-Crp4 and mature Crp4 interacted similarly with vesicles as their equivalent %CR values show. Consistent with mixed vesicle binding assays, (DE/G)-pro-Crp4-induced leakage from ani-

FIGURE 2. Sections from NOESYs of pro-Crp4<sup>20-92</sup>, pro-Crp4<sup>44-92</sup>, pro-Crp4<sup>54-92</sup>, and (DE/G)-pro-Crp4. Left column, CH<sub>α</sub>-CH NOEs typical for an antiparallel  $\beta$ -sheet, these show connectivities between residues 4–29 and 6–21. Middle column, CH<sub>β</sub>-CH<sub>β</sub> NOEs between residues 6 and 21. Right column, CH<sub>α</sub>-CH<sub>β</sub> NOEs from the  $\alpha$  of 11 to the  $\beta$ s of 28. Collectively, these and other NOEs confirm that pro-Crp4<sup>20-92</sup>, pro-Crp4<sup>44-92</sup>, pro-Crp4<sup>54-92</sup>, and (DE/G)-pro-Crp4 maintain both the disulfide pairings that characterize  $\alpha$ -defensins and the Crp4 secondary structure. Above each set of panels are the corresponding structural units from the NMR structure of Crp4 with the NOE connectivity indicated by a dashed line (1tv0.pdb (26)).



**FIGURE 3. Bactericidal activities of recombinant Crp4, pro-Crp4<sup>20-92</sup>, and pro-Crp4-processing intermediates.** Exponentially growing *S. aureus* (A), *L. monocytogenes* (B), and *S. Typhimurium*  $\Delta$ phoP (C) were exposed to the peptide concentrations shown at 37 °C in 50  $\mu$ l of PIPES-TSB buffer for 1 h (see "Experimental Procedures"). Following peptide exposure, the bacteria were plated on TSB-agar and incubated overnight at 37 °C. Surviving bacteria were counted as CFU/ml at each peptide concentration. Plate counts below  $1 \times 10^3$  CFU/ml signify that no colonies were counted. Symbols: pro-Crp4<sup>20-92</sup> (○), Crp4 (●), pro-Crp4<sup>44-92</sup> (▼), and pro-Crp4<sup>54-92</sup> (▽). The activities of MMP-7-processing intermediates were consistent against all bacteria tested.

onic membrane vesicles was similar to that of Crp4, greatly exceeding leakage induced by native pro-Crp4<sup>20-92</sup> exposure (Fig. 7B). Collectively, these results support the conclusion that acidic amino acid side chains in the N-terminal region of pro-Crp4<sup>20-92</sup> prevent the precursor's Crp4 moiety from interact-



**FIGURE 4. Processing intermediates are both membrane binding and membrane disruptive.** A, vesicles composed of DMPG/DMPC/PDA (1:1:3 mole ratio) were exposed to the peptides (see "Experimental Procedures") to test peptide-membrane interactions. The relative increase in %CR is proportional to the extent of bilayer disruption. B, increasing peptide concentrations were exposed to ANTS/DPX-loaded anionic vesicles and leakage of ANTS fluorophore was measured at 520 nm from quenched conditions. Replicate assays of membrane activity of each peptide correlated with bactericidal activity. Symbols: pro-Crp4<sup>20-92</sup> (○), Crp4 (●), pro-Crp4<sup>44-92</sup> (▲), and pro-Crp4<sup>54-92</sup> (△).

ing with anionic membranes, thereby blocking bactericidal activity by inhibiting interactions with the bacterial cell envelope.

**Recombinant Pro-Crp4<sup>44-92</sup>, Pro-Crp4<sup>54-92</sup>, and (DE/G)-pro-Crp4 Permeabilize Live *E. coli* ML35 Cells**—The relative membrane disruptive activities of pro-Crp4<sup>44-92</sup>, pro-Crp4<sup>54-92</sup>, and (DE/G)-pro-Crp4 also were compared with Crp4 and pro-Crp4<sup>20-92</sup> in *E. coli* cell permeabilization assays performed using 6, 3, and 1.5  $\mu$ M peptide concentrations. At all peptide concentrations, permeabilization induced by pro-Crp4<sup>44-92</sup> and pro-Crp4<sup>54-92</sup> were comparable to Crp4 controls (Fig. 8). (DE/G)-pro-Crp4 induced 86% the extent of Crp4 permeabilization activity at 60 min of peptide exposure but was the same as Crp4 by 120 min. The relative permeabilization data shown in Fig. 8 for 6  $\mu$ M peptide levels are representative of all peptide concentrations and are consistent with results of bactericidal peptide assays and phospholipid vesicle perturbation studies. Evidence of a low level of pro-Crp4<sup>20-92</sup>-induced *E. coli* permeabilization is apparent after 1 h (Fig. 8). Because low bactericidal activity can be detected at 15  $\mu$ M pro-

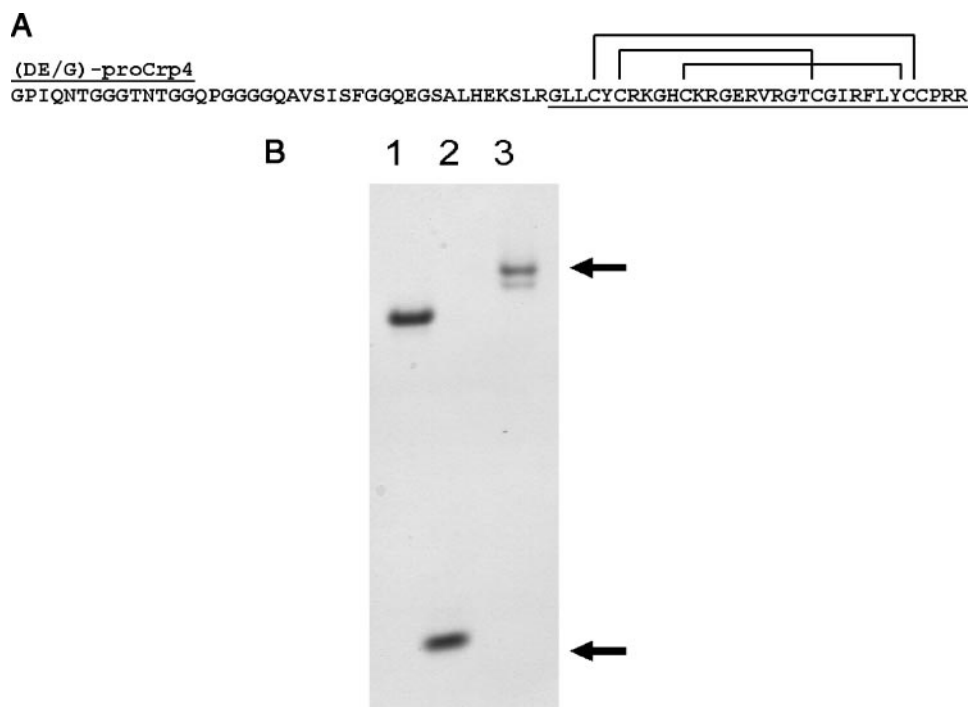


**FIGURE 5. Recombinant pro-Crp4<sup>20-92</sup>, Crp4, and (DE/G)-pro-Crp4.** *A*, the primary structure of the recombinant (DE/G)-pro-Crp4 is depicted. The underlining in the sequence signifies the fully processed Crp4 sequence. The disulfide connectivities are identified by the connecting bars above the sequence. *B*, 5- $\mu$ g samples of recombinant peptides depicted in *A* were resolved by AU-PAGE and stained with Coomassie Blue. Lanes: 1, (DE/G)-pro-Crp4; 2, Crp4 (lower arrow); and 3, pro-Crp4<sup>20-92</sup> (upper arrow).

Crp4<sup>20-92</sup> concentrations (Fig. 6), it may be that the native pro-Crp4<sup>20-92</sup> population may exist in equilibrium between partially membrane disruptive and inhibited forms.

**MMP-7 Activation of (DE/G)-pro-Crp4**—The acidic amino acids normally present in pro-Crp4<sup>20-43</sup> are not required for Crp4 folding (Fig. 2) or for MMP-7-mediated cleavage of pro-Crp4. Digestion of native pro-Crp4 with MMP-7 yields an intact Crp4<sup>59-92</sup> final product that has very similar mobility to Crp4 in AU-PAGE (14). Native Crp4 resists MMP-7 proteolysis completely due to the presence of the  $\alpha$ -defensin disulfide array (28). When (DE/G)-pro-Crp4 was incubated with MMP-7, the major final product of proteolysis was Crp4<sup>59-92</sup>, the same product of native pro-Crp4<sup>20-92</sup> processing by MMP-7 (Fig. 9A). The biochemically indistinguishable Crp4<sup>59-92</sup> products of pro-Crp4<sup>20-92</sup> and (DE/G)-pro-Crp4 MMP-7 processing are slightly less mobile than natural Crp4 in AU-PAGE (Fig. 9A), because complete Crp4 processing requires the removal of Leu<sup>59</sup> and Arg<sup>60</sup> to generate the Gly<sup>61</sup> N terminus of natural Crp4 (29). The aminopeptidase that catalyzes that reaction is unknown.

To determine whether mutagenesis of pro-Crp4<sup>20-43</sup> had effects on activation of bactericidal activity, Crp4, pro-Crp4, and (DE/G)-pro-Crp4 were exposed *in vitro* to MMP-7 and assayed for bactericidal activity against *E. coli* ML35. Mock digests lacking the convertase provided appropriate controls (Fig. 9B) (30, 31). As anticipated, the bactericidal activity of Crp4 digests was unaffected by incubation with MMP-7, and MMP-7 digestion of native pro-Crp4<sup>20-92</sup> activated bactericidal activity to a level equivalent to native Crp4 (14, 18). Also, MMP-7 digests of (DE/G)-pro-Crp4 were as active as

mock digests of the peptide, consistent with the activity of both forms being attributable to the Crp4 component of the precursor. Previous studies had established that the pro-Crp4 prosegment lacks antimicrobial activity in our *in vitro* assays (7), and MMP-7 itself is not bactericidal (6, 14). Because MMP-7 digests of pro-Crp4<sup>20-92</sup> still contain the pro-Crp4<sup>20-43</sup>, pro-Crp4<sup>44-53</sup>, and pro-Crp4<sup>54-58</sup> cleavage fragments, effective inhibition of pro-Crp4 bactericidal activity by the prosegment requires covalent association of pro-Crp4<sup>20-43</sup> with the Crp4 molecule.

## DISCUSSION

The pro-Crp4 proregion maintains the precursor molecule in an inactive state until MMP-7-mediated cleavage occurs at one of three sites. Recombinant peptides corresponding to MMP-7-processing intermediates have *in vitro* bactericidal activities that are equivalent to

that of native Crp4, identifying MMP-7 proteolysis at Ser<sup>43</sup> ↓ Ile<sup>44</sup> in pro-Crp4<sup>20-92</sup> as sufficient for activation. (DE/G)-pro-Crp4, prepared by substituting acidic amino acids N-terminal of Ser<sup>43</sup> with Gly, has bactericidal activity equivalent to that of Crp4, and (DE/G)-pro-Crp4 is processed normally by MMP-7 *in vitro*. In membrane binding and vesicle leakage assays, the native pro-Crp4-processing intermediates and (DE/G)-pro-Crp4 have membrane-disruptive activities similar to Crp4, sharply contrasting that of inactive pro-Crp4<sup>20-92</sup>. The active Crp4 intermediates appear to function by inducing graded leakage similar to Crp4 and not by alternative mechanisms potentially resulting from mutagenesis. Preliminary bactericidal peptide assays of (DE/NQ)-pro-Crp4<sup>20-92</sup>, a pro-Crp4 variant in which pro-Crp4<sup>20-43</sup> Asp and Glu residues were respectively converted to uncharged Asn and Gln, have shown that (DE/NQ)-pro-Crp4 and (DE/G)-pro-Crp4 are similar in activity. Thus, potential effects peculiar to Gly substitutions are excluded.<sup>3</sup> Collectively, these experiments strongly support the conclusion that acidic amino acids in pro-Crp4<sup>20-43</sup> block the bactericidal action of pro-Crp4 by inhibiting membrane-disruptive behavior. It is the presence of acidic amino acids in the prosegment rather than the absolute length of the peptide extension bound to the Crp4 N terminus that inhibits pro-Crp4 membrane-disruptive behavior and microbicidal action.

NMR results confirm that the defensin domain folds correctly in the absence of acidic residues within the proregion. In

<sup>3</sup> C. S. Weeks, S. Figueredo, and A. J. Ouellette, unpublished observation.

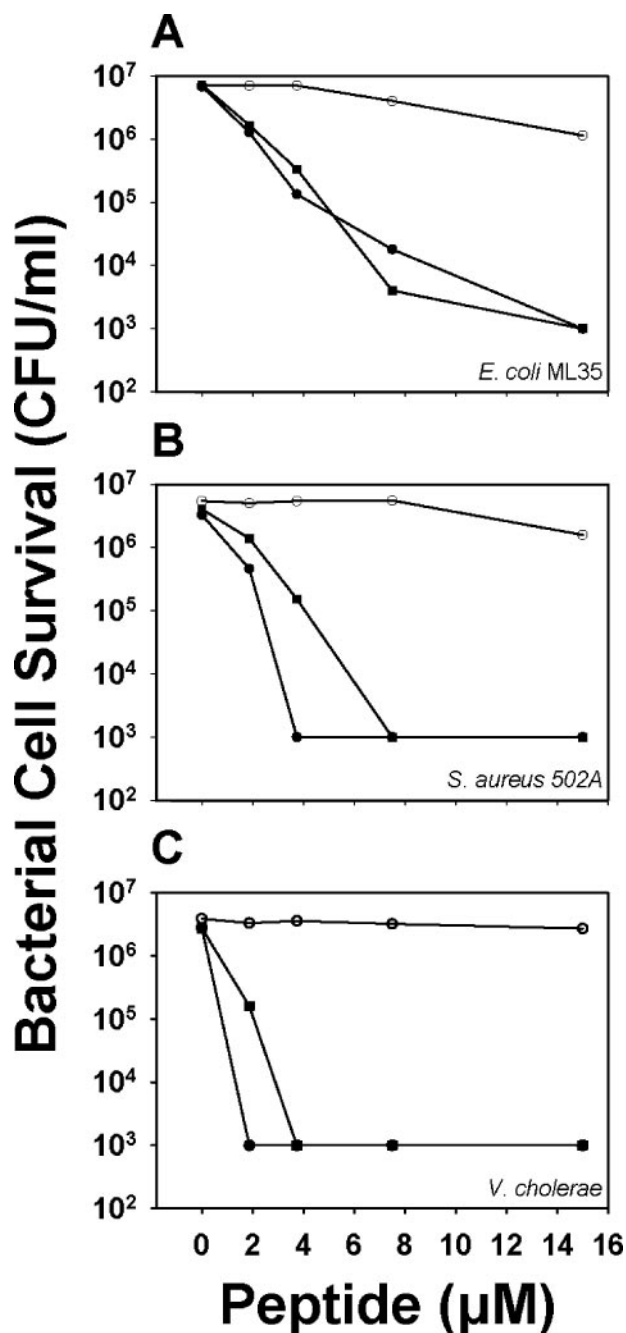


FIGURE 6. Bactericidal activity of recombinant Crp4, pro-Crp4<sup>20-92</sup>, and (DE/G)-pro-Crp4. Exponentially growing *E. coli* ML35 (A), *S. aureus* 502A (B), and *V. cholerae* (C) were exposed to the peptides, and surviving bacteria were quantified as CFU/ml. Symbols: Crp4 (●), pro-Crp4<sup>20-92</sup> (○), and (DE/G)-pro-Crp4 (■). (DE/G)-pro-Crp4 exhibits activity equivalent to Crp4 in replicate bactericidal assays.

fact, comparison of NMR chemical shifts shows essentially no change between defensin peak positions of pro-Crp4<sup>44-92</sup>, pro-Crp4<sup>54-92</sup>, (DE/G)-pro-Crp4, and Crp4. In contrast, the defensin domain of native pro-Crp4<sup>20-92</sup> does show backbone chemical shift changes that are consistent with Crp4 interactions of the prosegment.<sup>4</sup> Thus the pro-region of the DE/G variant no longer masks the intact Crp4  $\alpha$ -defensin sufficiently to inactivate the molecule. We speculate that direct interactions

<sup>4</sup> M. J. Cocco, C. S. Weeks, and A. J. Ouellette, unpublished observation.

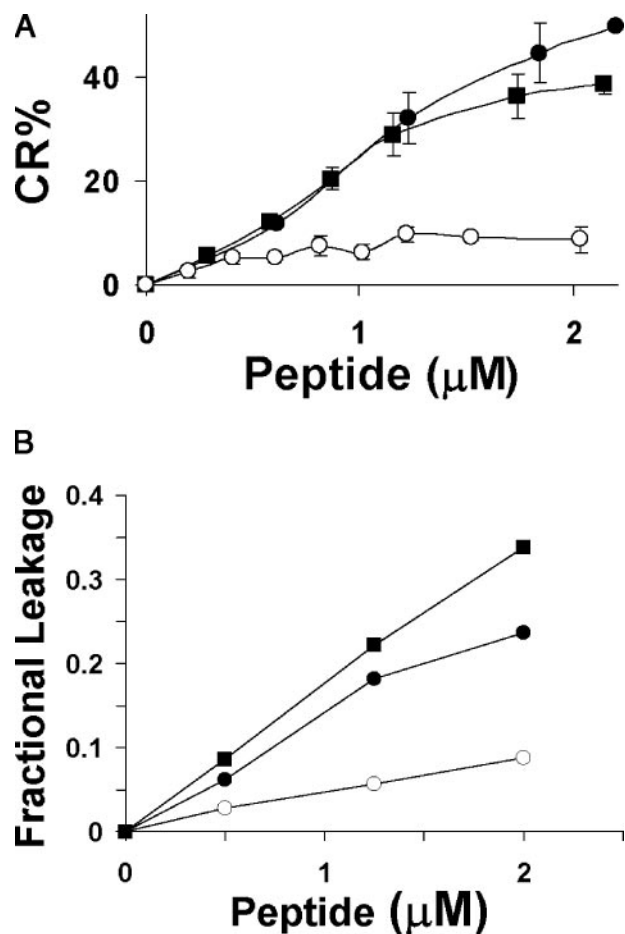


FIGURE 7. (DE/G)-pro-Crp retains membrane-binding and membrane-disruptive properties. A, vesicles composed of DMPG/DMPC/PDA (1:1:3 mole ratio) were exposed to the peptides (see "Experimental Procedures") to test peptide-membrane interactions. The relative increase in %CR is proportional to the extent of bilayer disruption. B, increasing peptide concentrations were exposed to ANTS/DPX-loaded anionic vesicles, and leakage of ANTS fluorophore was measured at 520 nm from quenched conditions. Membrane activity of each peptide correlated with bactericidal activity. Symbols: Crp4 (●), pro-Crp4<sup>20-92</sup> (○), and (DE/G)-pro-Crp4 (■).

between Arg residues, critical for Crp4 bactericidal activity (20), and acidic residues in the prosegment may be evident in the pro-Crp4 solution structure. Also, the amino acid composition of prosegment residue positions 40-59 may contribute appropriate spacing and side-chain composition to provide optimal interactions between the anionic pro-Crp4<sup>20-43</sup> region and the Crp4 peptide.

One possible role of the prosegment is to minimize potential cytotoxicity or membrane-disruptive behavior of  $\alpha$ -defensin peptides in the biosynthetic pathway. For example, certain tumor cells and also nonmalignant cells undergo cytolysis when exposed to  $\alpha$ -defensins from human and rabbit granulocytes (32, 33). HNP3 from polymorphonuclear leukocytes are cytotoxic to human lung fetal fibroblast MRC-5 cells, A549 lung adenocarcinoma cells, and human umbilical vein endothelial cell primary cultures (34). By inhibiting  $\alpha$ -defensin-induced membrane disruption, the prosegment may prevent deleterious effects to the host cell during pro- $\alpha$ -defensin biosynthesis, folding, and packaging into granules. Mouse Crp4 has markedly greater affinity for anionic phospholipid bilayers than for neu-

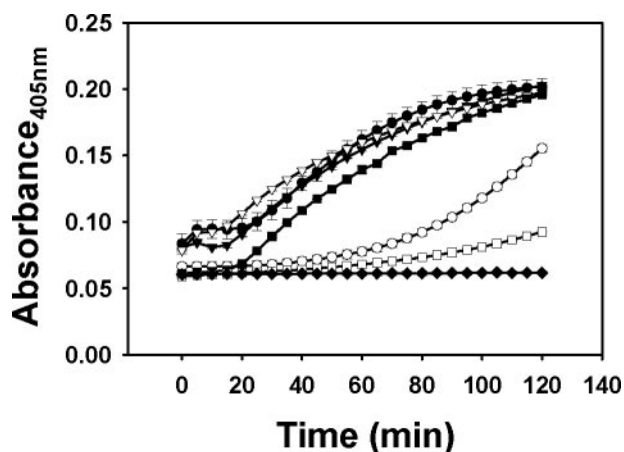


FIGURE 8. *E. coli* ML35 permeabilization by Crp4, pro-Crp4<sup>20-92</sup>, and (DE/G)-pro-Crp4. *E. coli* ML35 growing in log-phase was exposed to 6  $\mu$ M peptide concentrations in the presence of ONPG at 37 °C. ONPG hydrolysis was measured to determine the amount of permeabilization caused by the experimental peptides. Symbols: pro-Crp4<sup>20-92</sup> (○), Crp4 (●), pro-Crp4<sup>44-92</sup> (▼), pro-Crp4<sup>54-92</sup> (▽), (DE/G)-pro-Crp4 (■), ONPG (□), and ONPG and bacteria (◆).

tral model membranes that more closely resemble mammalian plasma membranes. Nevertheless, the prosegment may inhibit  $\alpha$ -defensin precursors from inserting into the *cis*- and *trans*-Golgi prior to being sequestered into secretory granules (7). Human Paneth cells store  $\alpha$ -defensins as proforms, which are cleaved by trypsin after secretion into the gut lumen, a further suggestion that inhibition of defensin-mediated intracellular membrane disruption may be under positive selection. Although  $\alpha$ -defensins in the gut lumen may potentially be cytotoxic to epithelial cells after secretion, preliminary data show that pro-Crp4<sup>20-92</sup> and Crp4 are not cytotoxic to human fibroblast cell line HS68 at 25  $\mu$ M.<sup>5</sup> Although mouse Crps are released in millimolar concentrations at the point of secretion (3), peptide concentrations may dissipate rapidly as granules dissolve and peptides diffuse from the crypt compartment to the markedly greater volume of the small intestinal lumen above the crypt-villus boundary.

The pro-Crp4 prosegment efficiently inhibits the bactericidal activity of the C-terminal Crp4  $\alpha$ -defensin moiety only when present in *cis* and covalently bound in the precursor molecule. When pro-Crp4<sup>20-92</sup> is cleaved by MMP-7 and tested for *in vitro* bactericidal activity, the combined products of the cleavage reaction are equivalent in activity to Crp4 peptide controls, even though the cleaved prosegment products remain in solution at equimolar concentrations. HNP-1 has been shown to interact with its soluble propeptide in *trans* as evidenced by decreased peptide fluorescence and coincident with a blue shift (35). At proregion concentrations of maximal prosegment inhibition of HNP-1, significant HNP-1 bacteriostatic activity was retained in comparison with full-length pro-HNP-1 (36). Crp4 also is inhibited by its prosegment when incubated in *trans* (7), but the proregion inhibition of Crp4 bactericidal activity is only 2-fold rather than the 1000-fold difference between Crp4 and native, full-length pro-Crp4<sup>20-92</sup> (14). Although HNP-1 bound to soluble propeptide in *trans* and partially inhibited bactericidal activity, we speculate that components of the bacterial cell

<sup>5</sup> C. S. Weeks, D. Tran, and A. J. Ouellette, unpublished observation.

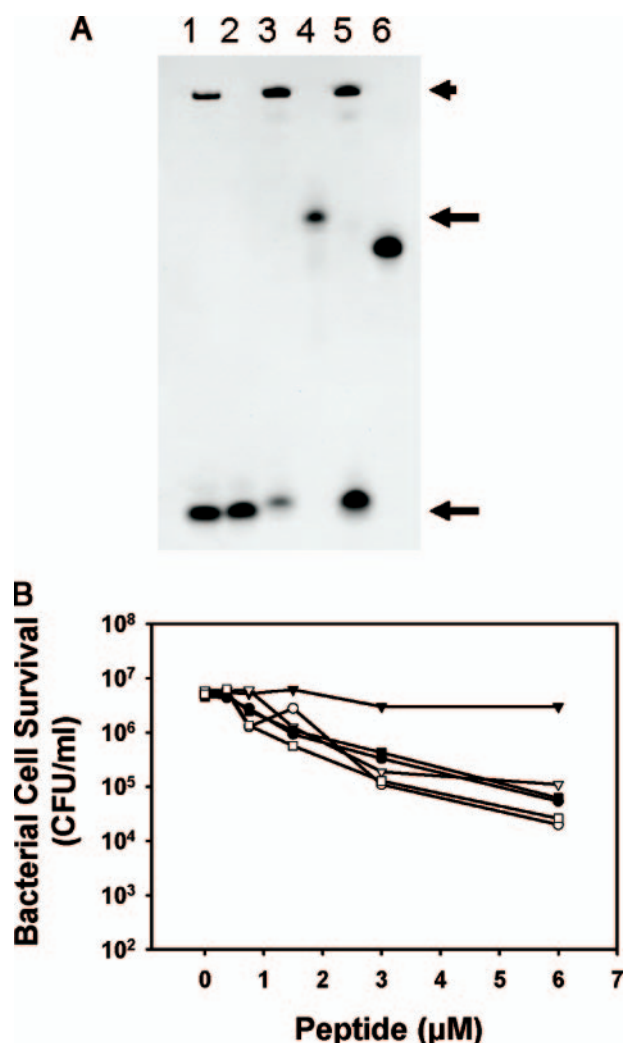


FIGURE 9. MMP-7 cleavage of Crp4, pro-Crp4<sup>20-92</sup>, and (DE/G)-pro-Crp4 and activity of the cleavage products. **A**, 10- $\mu$ g of recombinant Crp4, pro-Crp4<sup>20-92</sup>, and (DE/G)-pro-Crp4 were incubated with or without 0.5 M equivalents of MMP-7 in HEPES buffer for 18 h at 37 °C (see "Experimental Procedures"). The digests were resolved on AU-PAGE and stained with Coomassie Blue. The small arrow delineates the MMP-7 band in lanes 1, 3, and 5. Lanes: 1, Crp4 plus MMP-7; 2, Crp4 (lower arrow); 3, pro-Crp4<sup>20-92</sup> plus MMP-7; 4, pro-Crp4<sup>20-92</sup> (upper arrow); 5, (DE/G)-pro-Crp4 plus MMP-7; 6, (DE/G)-pro-Crp4. **B**, 15  $\mu$ M samples of pro-Crp4<sup>20-92</sup>, Crp4, and (DE/G)-pro-Crp4 were digested as described and exposed to *E. coli* ML35 in the concentrations shown. Bacteria were plated, and surviving bacteria were quantified as CFU/ml. Symbols: Crp4 (●), Crp4 plus MMP-7 (○), pro-Crp4<sup>20-92</sup> (▼), pro-Crp4<sup>20-92</sup> plus MMP-7 (▽), (DE/G)-pro-Crp4 (■), and (DE/G)-pro-Crp4 plus MMP-7 (□). MMP-7 cleavage does not require the acidic residues in pro-Crp4<sup>20-43</sup> for processing of pro-Crp4<sup>20-92</sup>.

envelope may have greater affinity for the HNP-1 than for binding to prosegment in solution. Activated Crps and prosegments co-localize in Paneth cell granules, and the majority of pro-Crps are activated before or during granulogenesis (7), resulting in the secretion of both Crps and prosegment proteolytic fragments into the small intestinal lumen. Because MMP-7-generated prosegment fragments lose inhibitory activity once cleaved from the  $\alpha$ -defensin peptide component of the proform, we infer that secreted Crps will be active following secretion despite the presence of potentially inhibitory proregion fragments. However, if post-translational processing of pro- $\alpha$ -defensins were defective, the covalently linked proregion would

remain in proximity and inhibit Crp interactions with target cells. The phenotype of MMP-7-null mice is characterized by a lack of processed Crps and increased susceptibility to oral bacterial infection (6). We speculate that human populations with corresponding defects in pro- $\alpha$ -defensin activation also may have impaired enteric immunity and be predisposed to mucosal infections and inflammation.

*Acknowledgment*—We thank Drs. Hans Vogel and Michael E. Selsted for useful discussions.

## REFERENCES

1. Selsted, M. E., and Ouellette, A. J. (2005) *Nat. Immunol.* **6**, 551–557
2. Zasloff, M. (2002) *Nature* **415**, 389–395
3. Ayabe, T., Satchell, D. P., Wilson, C. L., Parks, W. C., Selsted, M. E., and Ouellette, A. J. (2000) *Nat. Immunol.* **1**, 113–118
4. Clarke, L. L., Gawenis, L. R., Bradford, E. M., Judd, L. M., Boyle, K. T., Simpson, J. E., Shull, G. E., Tanabe, H., Ouellette, A. J., Franklin, C. L., and Walker, N. M. (2004) *Am. J. Physiol.* **286**, G1050–G1058
5. Norkina, O., Burnett, T. G., and De Lisle, R. C. (2004) *Infect. Immun.* **72**, 6040–6049
6. Wilson, C. L., Ouellette, A. J., Satchell, D. P., Ayabe, T., Lopez-Boado, Y. S., Stratman, J. L., Hultgren, S. J., Matrisian, L. M., and Parks, W. C. (1999) *Science* **286**, 113–117
7. Ayabe, T., Satchell, D. P., Pesendorfer, P., Tanabe, H., Wilson, C. L., Hagen, S. J., and Ouellette, A. J. (2002) *J. Biol. Chem.* **277**, 5219–5228
8. Salzman, N. H., Ghosh, D., Huttner, K. M., Paterson, Y., and Bevins, C. L. (2003) *Nature* **422**, 522–526
9. Ghosh, D., Porter, E., Shen, B., Lee, S. K., Wilk, D., Drazba, J., Yadav, S. P., Crabb, J. W., Ganz, T., and Bevins, C. L. (2002) *Nat. Immunol.* **3**, 583–590
10. Daher, K. A., Lehrer, R. I., Ganz, T., and Kronenberg, M. (1988) *Proc. Natl. Acad. Sci. U. S. A.* **85**, 7327–7331
11. Michaelson, D., Rayner, J., Couto, M., and Ganz, T. (1992) *J. Leukoc. Biol.* **51**, 634–639
12. Valore, E. V., and Ganz, T. (1992) *Blood* **79**, 1538–1544
13. Liu, L., and Ganz, T. (1995) *Blood* **85**, 1095–1103
14. Shirafuji, Y., Tanabe, H., Satchell, D. P., Henschen-Edman, A., Wilson, C. L., and Ouellette, A. J. (2003) *J. Biol. Chem.* **278**, 7910–7919
15. Putsep, K., Axelsson, L. G., Boman, A., Midtvedt, T., Normark, S., Boman, H. G., and Andersson, M. (2000) *J. Biol. Chem.* **275**, 40478–40482
16. Wimley, W. C., Selsted, M. E., and White, S. H. (1994) *Protein Sci.* **3**, 1362–1373
17. Hristova, K., Selsted, M. E., and White, S. H. (1996) *Biochemistry* **35**, 11888–11894
18. Satchell, D. P., Sheynis, T., Shirafuji, Y., Kolusheva, S., Ouellette, A. J., and Jelinek, R. (2003) *J. Biol. Chem.* **278**, 13838–13846
19. Satchell, D. P., Sheynis, T., Kolusheva, S., Cummings, J., Vanderlick, T. K., Jelinek, R., Selsted, M. E., and Ouellette, A. J. (2003) *Peptides* **24**, 1795–1805
20. Tanabe, H., Qu, X., Weeks, C. S., Cummings, J. E., Kolusheva, S., Walsh, K. B., Jelinek, R., Vanderlick, T. K., Selsted, M. E., and Ouellette, A. J. (2004) *J. Biol. Chem.* **279**, 11976–11983
21. Kolusheva, S., Shahal, T., and Jelinek, R. (2000) *Biochemistry* **39**, 15851–15859
22. Smolarsky, M., Teitelbaum, D., Sela, M., and Gitler, C. (1977) *J. Immunol. Methods* **15**, 255–265
23. Cummings, J., Satchell, D., Shirafuji, Y., Ouellette, A., and Vanderlick, T. (2003) *Aust. J. Chem.* **56**, 1031–1034
24. Piatto, M., Saudek, V., and Sklenar, V. (1992) *J. Biomol. NMR* **2**, 661–665
25. Delaglio, F., Grzesiek, S., Vuister, G. W., Zhu, G., Pfeifer, J., and Bax, A. (1995) *J. Biomol. NMR* **6**, 277–293
26. Jing, W., Hunter, H. N., Tanabe, H., Ouellette, A. J., and Vogel, H. J. (2004) *Biochemistry* **43**, 15759–15766
27. Jelinek, R., and Kolusheva, S. (2001) *Biotechnol. Adv.* **19**, 109–118
28. Maemoto, A., Qu, X., Rosengren, K. J., Tanabe, H., Henschen-Edman, A., Craik, D. J., and Ouellette, A. J. (2004) *J. Biol. Chem.* **279**, 44188–44196
29. Selsted, M. E., Miller, S. I., Henschen, A. H., and Ouellette, A. J. (1992) *J. Cell Biol.* **118**, 929–936
30. Fields, P. I., Groisman, E. A., and Heffron, F. (1989) *Science* **243**, 1059–1062
31. Miller, S. I., Pulkkinen, W. S., Selsted, M. E., and Mekalanos, J. J. (1990) *Infect. Immun.* **58**, 3706–3710
32. Lichtenstein, A., Ganz, T., Selsted, M. E., and Lehrer, R. I. (1986) *Blood* **68**, 1407–1410
33. Lichtenstein, A. K., Ganz, T., Nguyen, T. M., Selsted, M. E., and Lehrer, R. I. (1988) *J. Immunol.* **140**, 2686–2694
34. Okrent, D. G., Lichtenstein, A. K., and Ganz, T. (1990) *Am. Rev. Respir. Dis.* **141**, 179–185
35. Wu, Z., Prah, A., Powell, R., Ericksen, B., Lubkowski, J., and Lu, W. (2003) *J. Pept. Res.* **62**, 53–62
36. Valore, E. V., Martin, E., Harwig, S. S., and Ganz, T. (1996) *J. Clin. Invest.* **97**, 1624–1629